THE UNIVERSITY of EDINBURGH

Edinburgh Research Explorer

Thin Polymer Film Force Spectroscopy: Single Chain Pull-out and Desorption

OPEN ACCESS

Thin Polymer Film Force Spectroscopy: Single Chain Pull-out and Desorption

Jake McClements* and Vasileios Koutsos*

School of Engineering, Institute for Materials and Processes, The University of Edinburgh, Sanderson Building, King's Buildings, Edinburgh EH9 3FB, United Kingdom

ABSTRACT: Atomic force microscopy (AFM) was utilized to investigate the force associated with chain pull-out and single chain desorption of poly(styrene-co-butadiene) random copolymer thin films on mica, silicon and graphite substrates. Chain pull-out events were common and produced a force of 20 - 25 pN. The polymer desorption force was strongest on the graphite substrate and weakest on the mica, which agreed with the calculated work of adhesion for each system and the substrate hydrophobicity. Furthermore, it was demonstrated that there was a systematic order to when each of these phenomena occurred during the tip retraction from the surface, which provided information about the structure of the thin films.

Understanding polymer adhesion at the molecular level is vitally important for fundamental polymer science,[1] but also to many applications such as advanced composite materials, [2–4] polymer coatings[5,6] and adhesives.[7] In all cases, there is a critical interface where individual chains are in contact with a rigid substrate. AFM can be used to perform single molecule force spectroscopy (SMFS) experiments which can investigate the forces associated with single polymer chain adhesion and desorption at the nanoscale.[8,9]

Despite the wide array of SMFS experiments carried out on polymers in recent years,[10–12] the extraction of chains from a thin polymer film where there exists a competition between chain pull-out and desorption events remains unexplored. This is an important area for many synthetic polymers as such molecular phenomena underpin their adhesive properties.[6,13,14] With the growing usage of carbon-based particles for advanced polymer composites,[4,15,16] this is particularly important for polymer films formed on carbon substrates, such as graphite.

In this paper, AFM SMFS was employed to investigate the specific interactions between poly(styrene-co-butadiene) random copolymer (SBR) chains and mica, silicon and graphite substrates. SBR is used in many applications, such as composite materials and adhesives.[17] For example, carbon black is regularly combined with SBR in the manufacture of automotive tires. A blank AFM tip was used to pick up and pull polymer chains from thin SBR films on each substrate and the resulting force-separation profiles were analyzed to provide quantitative information. The results identify the force associated with single polymer chain desorption from each substrate and the silicon AFM tip, as well as, the force associated with single chain pull-out from the SBR films. Furthermore, a systematic order to when each of these phenomena occurred during retraction from the surface was identified.

All experiments were carried out using a SBR random copolymer (Michelin) with a molecular weight of 355 kg/mol. The SBR was monodisperse (Đ = 1.02), with a styrene-butadiene ratio of 25.9:74.1 and a T_g of -35.4 °C. Mica, silicon and graphite substrates were manually dip-coated (60 minute incubation) in toluene/SBR solutions (6.95 mg/ml) to create thin polymer films. The mica and graphite substrates were cleaved with tape immediately before dip-coating. The silicon substrate was washed with acetone and ethanol. After removal from the solution, each substrate was dried with nitrogen for 2 minutes and left to dry for approximately 16 hours before use.

All AFM imaging and force spectroscopy was carried out using a Bruker Multimode/Nanoscope IIIa under ambient conditions. Details of the AFM imaging can be found in previous articles.[18–21] In the force spectroscopy experiments, Bruker MSNL-10 tips which were composed of silicon with a thin native oxide layer and had spring constants of 0.01 N/m were used. Similarly to the silicon substrates, the AFM tips were washed in acetone and ethanol before use. The approach/retract velocity of the AFM tips during

the experiments was 1.5 μm/s. The polymer films were characterized using AFM imaging (see Supporting Information). The SBR film thicknesses (measured using AFM) were estimated at 31 ± 9 nm, 39 ± 9 nm and 27 ± 8 nm on the mica, silicon and graphite substrates, respectively. Contact angle goniometry was performed using a KRÜSS Drop Shape Analyzer DSA30S at ambient temperatures.

During the experiments, each approach/retract cycle of the AFM tip produced a force-separation profile (Figure 1). The profiles were similar for the experiments on each substrate and exhibited an unspecific-interaction adhesive minimum at low tip-sample separations. However, as tip-sample separation increased, fewer polymer chains remained bridged between the tip and surface, which allowed for single chain events to be observed. These events were characterized by force plateaus and steps which are associated with chain desorption from the tip/substrates and chain pull-out.
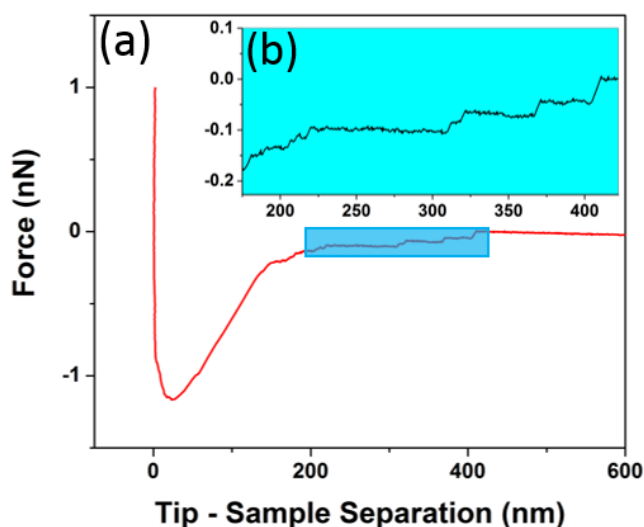

Figure 1. (a) Typical force-separation profile for SBR on the silicon substrate. (b) Zoomed section which shows force steps and plateaus. The zoomed area is represented by the blue box in (a).

Figure 2 presents histograms which show the distributions of step force values on each substrate. All histograms have a number of distinct peaks which represent the forces associated with the three different phenomena which occurred. These are polymer desorption from the tip, polymer desorption from each substrate and chain pull-out. All the histograms have two distinct common features: a main peak at 20 - 25 pN and a secondary peak at 55 - 60 pN. As these peaks are in the same (force) position for each histogram, they cannot represent desorption from the three substrates as they have distinctly different surface properties. Therefore, they must represent the forces associated with chain pull-out and desorption from the tip as these phenomena should have the same step force values on each substrate.
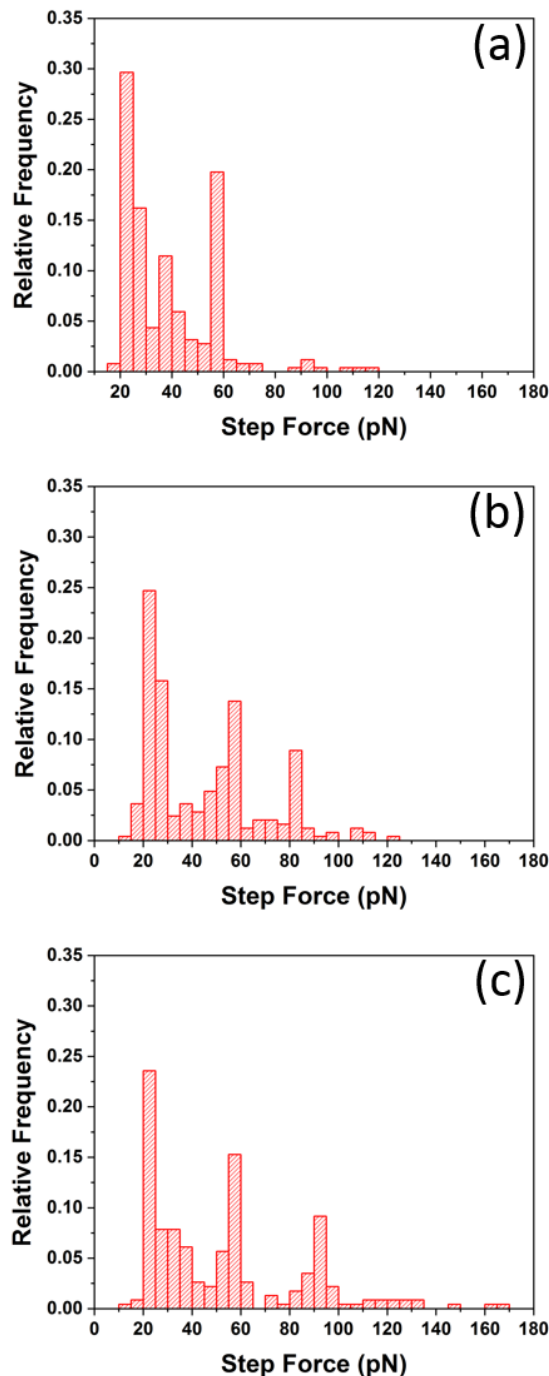

Figure 2. Histograms showing the step force distributions for each substrate: (a) mica, (b) silicon, (c) graphite.

The force associated with chain pull-out can be estimated using (see also Supporting Information for details on chain pull-out forces):[22–24]

$$F_{pull-out} = 2\pi r \gamma \qquad (1)$$

2

where r is the chain radius (estimated at 0.15 nm), and γ is the surface energy of the polymer (39 mJ/m^2 and 31 mJ/m^2 for polystyrene and polybutadiene, respectively).[22,25–27] Taking into account the polymer's styrene-butadiene ratio, the force associated with chain pull-out was estimated at 31 pN which is close to the value of the primary peak in each histogram. Furthermore, previous AFM investigations estimated the force associated with chain pull-out to generally range from 15 to 40 pN.[6,23,27,28] Therefore, the peak at 20 – 25 pN can be associated with chain pull-out and relevant polymer-polymer interactions. Consequently, the other common peak in each histogram at 55 - 60 pN represents the force associated with polymer desorption from the tip. It was calculated that the force contribution due to single chain friction was negligible and therefore, could be omitted from the results (see Supporting Information).

The histograms for the silicon and graphite substrates (Figures 2b and 2c) also have a third distinct peak with a larger force value (80 - 85 pN and 90 - 95 pN for the silicon and graphite, respectively). As these peaks have different force values on the silicon and graphite, they likely represent polymer desorption from each substrate. Furthermore, these peaks have low relative frequencies which is expected as desorption from the strongly adsorbing substrates should have the lowest probability of occurring. Whilst it is clear that the peaks at 80 - 85 pN and 90 - 95 pN on the silicon and graphite histograms are *related to* substrate desorption, it is an oversimplification to present these values as the actual polymer desorption forces from each substrate. This is because when a chain segment is desorbed from a substrate surface, the chain is still embedded within the polymer film and experiences polymer/polymer interactions until it is completely removed from the film. As substrate desorption and chain pull-out occur simultaneously for these polymers, they are represented by a single step. Therefore, the respective peaks at 80 - 85 pN and 90 - 95 pN in the silicon and graphite histograms actually represent the force associated with substrate desorption, in addition to, chain pull-out. Thus, to obtain an accurate force for the substrate desorption, the chain pull-out (20 - 25 pN) must be subtracted from the force of the peaks. Consequently, the true desorption forces are estimated at 55 - 65 pN and 65 - 75 pN for the silicon and graphite substrates, respectively.

The forces associated with polymer desorption from the silicon tip and silicon substrate are 55 - 60 pN and 55 - 65 pN, respectively. The force values are very similar which is expected as both the tip and substrate are composed of silicon with a thin oxide layer. The slightly larger desorption force for the silicon substrate is likely due to a small difference in the oxide layer thickness on each surface, or to the large curvature of the tip which can lead to reduced interfacial contact with the SBR chains.[29,30]

We would expect that desorption from the tip (55 - 60 pN) would be most prevalent on the strongly adsorbing substrates. However, this is not the case, as the peak at 55

- 60 pN has the largest relative frequency on the weakly adsorbing mica substrate (0.20 versus 0.15). This suggests that this peak in the mica histogram (Figure 2a) represents the force associated with two separate phenomena with similar force values which form a single peak with a larger relative frequency. Consequently, it appears that the peak at 55 - 60 pN actually represents the force associated with desorption from the tip, as well as, substrate desorption/chain pull-out. Therefore, after the subtraction of 20 - 25 pN due to polymer-polymer interactions, the desorption force on the mica is calculated as 30 - 40 pN. Table 1 presents the force values of each interaction measured during the experiments.

Table 1. The force values of each interaction.

Interaction	Force (pN)
SBR - SBR	20 - 25
SBR - Mica	30 - 40
SBR - Silicon Tip	55 - 60
SBR - Silicon	55 - 65
SBR - Graphite	65 - 75

On the histogram for the mica (Figure 2a), there is also a smaller peak with a value of 35 - 40 pN. Interestingly, the peak has a very similar value to the force of SBR desorption from the mica substrate (30 - 40 pN). This suggests that the peak represents a phenomenon where the SBR chains are desorbed from the substrate, but are not completely removed from the film. This is more likely to occur when the polymer chains have long loop and tail conformations next to trains, i.e. adsorbed chain segments.[31,32] The desorption of a train segment will result in a step with a value equal to the force associated with substrate desorption, as long as, the rest of the polymer chain is still adsorbed to the substrate (by other segments) and at the same time still embedded within the film. Such desorption of individual train segments is fairly common on the mica, but not on the silicon or graphite. This is because on weakly adsorbing substrates (mica), the chains form a greater number of loop and tail conformations.[31] This demonstrates the capability of AFM force spectroscopy to reveal important information regarding the conformational properties of polymer chains within thin films.

The ranking of polymer desorption force values on the mica and graphite agree with our previous AFM imaging observations.[18,19] In the experiments, the SBR weakly adsorbed to the mica and formed spherical-cap shaped nanodroplets with large contact angles.[18] Whereas on the graphite, the polymer was more strongly adsorbed and formed structures with lower contact angles, such as networks and nanoribbons.[19] The work of adhesion between

the SBR films and each substrate is also calculated and compared with the desorption force values (Table 2). In order to calculate the work of adhesion, the interfacial energy ($\gamma_{i,j}$) of each system was first calculated using the Owens and Wendt equation:[33,34]

$$\gamma_{i,j} = \gamma_i + \gamma_j - 2\sqrt{\gamma_i^p \gamma_j^p} - 2\sqrt{\gamma_i^d \gamma_j^d} \qquad (2)$$

where γ is the total surface energy, γ^p is the polar component of surface energy and γ^d is the dispersive component of surface energy of materials i and j. The surface energy values were taken from the literature and are included in the Supporting Information.[33,35–37] The work of adhesion (W_a) between the SBR film and each substrate was estimated using the following equation:[38]

$$W_a = \gamma_i + \gamma_j - \gamma_{i,j} \qquad (3)$$

The calculated work of adhesion was largest for the graphite and smallest for the mica (Table 2). These results correlate with the measured polymer desorption force of each substrate. Furthermore, the desorption force values also correlate to the water contact angles of each substrate which are < 5°, 46° and 84 - 86° for the mica, silicon and graphite, respectively.[39,40] The measured polymer desorption force was largest on the most hydrophobic substrate (graphite) and smallest on the least hydrophobic substrate (mica).

TABLE 2. The polymer desorption force and work of adhesion of each substrate/system.

Substrate	Desorption Force (pN)	Work of Adhesion (mJ/m²)
Mica	30 - 40	58
Silicon	55 - 65	62
Graphite	65 - 75	68

The initial force steps in each profile generally have smaller magnitudes compared to the final force steps. This is clearly observed in Figure 3. This trend indicates that the initial force steps and final force steps represent different physical phenomena.
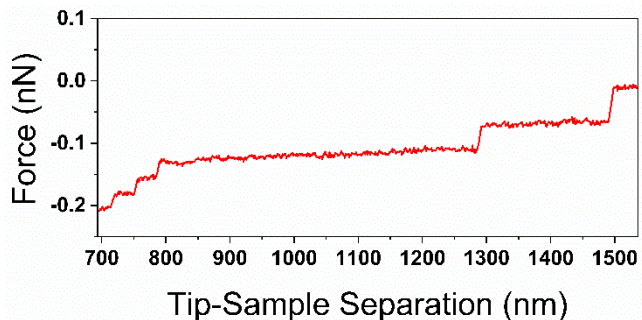

Figure 3. A section of a typical force-separation profile for SBR on mica. The force steps at lower tip-sample separations (700 - 800 nm) have a smaller magnitude, whereas the force steps at higher tip-sample separations (1300 - 1500 nm) have a larger magnitude.

Figure 4 presents histograms which show the magnitude of the first force step (lower separations) and the final force step (higher separations) in the profiles for each substrate. The histograms in Figures 4a, 4c and 4e show the distributions for the first force step on each substrate, and they all exhibit a main peak with a value of 20 - 25 pN. Therefore, this demonstrates that the first step in the profiles mainly represent the force associated with chain pull-out. Figures 4b, 4d and 4f show the magnitude of the final force step in the profiles for each substrate. The histogram for the mica (Figure 4b) has a single distinct peak at 55 - 60 pN with a high relative frequency. As aforementioned, this peak is associated with desorption from the tip, as well as, simultaneous desorption from the mica substrate/polymer film. The histograms for the silicon and graphite substrates (Figures 4d and 4f) each have two distinct peaks with lower relative frequencies. The peaks have values of 55 - 60 pN and 80 - 85 pN on the silicon, and 55 - 60 pN and 90 - 95 pN on the graphite. The peaks at 55 - 60 pN represent polymer desorption from the tip, whereas the peaks with larger force values represent simultaneous chain desorption from the silicon/graphite and chain pull-out.
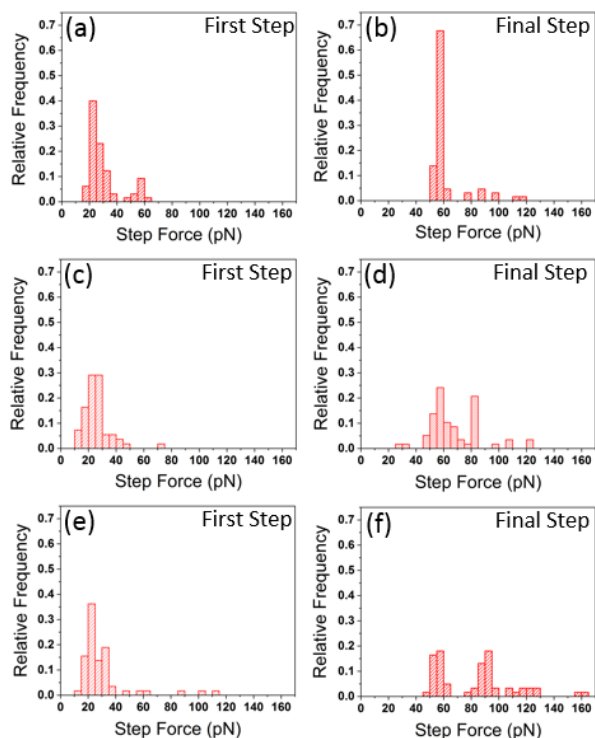
4

Figure 4. Histograms showing the step force distributions for the first and final step in the force-separation profiles for each substrate: (a) mica - first step, (b) mica - final step, (c) silicon - first step, (d) silicon - final step, (e) graphite - first step, (f) graphite - final step.

The results in Figure 4 demonstrate that there is a distinct order to when each phenomena typically occurs during the tip retraction. The first force step represents chain pull-out, which likely occurs as polymer chains near the free thin film surface are not adsorbed to the substrate. In contrast, the final force steps appear to almost exclusively represent desorption from the tip/substrates. These force spectroscopy results provide an insight into the structure of the thin film; they imply two populations of chains: 1) a population of chains near the polymer film surface with almost no adsorbed segments on the substrate, (2) a population of chains closer to the base of the film with a large proportion of their length adsorbed to the substrate. The existence of different populations of chains is highly dependent on film thickness.[41] Polymer chains can have different properties depending on where they are located within a thin film. For example, experimental and simulation studies have demonstrated that the T_g and elastic modulus of a polymer thin film can be larger at the base of a film where the chains are strongly anchored, compared to the film's surface where the chains can move more freely.[41–43] The existence of two populations of chains provides new insight into these phenomena.

We have utilized AFM force spectroscopy to investigate single chain pull-out and substrate desorption in SBR thin films. Chain pull-out from the thin films produced a force of 20 – 25 pN and was the most common event. The force of polymer desorption from mica, silicon and graphite was found to be substrate dependent with values of 30 - 40 pN, 55 - 65 pN and 65 - 75 pN, respectively. The polymer desorption force was weakest on the mica, and strongest on the graphite which correlated with previous AFM imaging observations, the water contact angle of each substrate and the calculated work of adhesion for each system. We showed that usually the desorbed chains are also pulled out from the thin films and generally one has to account for the pull-out force in order to accurately calculate the desorption force. However, in the case of weakly adsorbed substrates such as mica, there are some chains with train sections which can be individually desorbed from the substrate's surface without the full chains being pulled out of the thin film. The polymer desorption force from the silicon AFM tip and silicon substrate were similar to one another and the small deviation was likely due to differences in their native oxide layer thicknesses or to the large surface curvature of the tip. The force spectroscopy results also demonstrated that there was a systematic order to when the different phenomena occurred during the tip retraction. The first force step in each profile generally represented chain pull-out, whereas the final force step typically represented polymer desorption from the substrate/tip. These results provide useful insight regarding the structure of the thin films and how this influences adhesion and desorption behavior at the nanoscale.

ASSOCIATED CONTENT

Supporting Information.
Details of optimizing the experimental procedure, AFM images of SBR films on each substrate, calculations of the contribution to adhesion by friction and surface energy values for each component.

This material is available free of charge via the Internet at http://pubs.acs.org.

AUTHOR INFORMATION

Corresponding Authors

*E-mail: mcclements.j@gmail.com
*E-mail: vasileios.koutsos@ed.ac.uk

Notes
The authors declare no competing financial interest.

REFERENCES

(1) Israelachvili, J. N. *Intermolecular and Surface Forces*, second ed.; Academic Press: New York City, 1992.

(2) Mamalis, D.; Murray, J. J.; McClements, J.; Tsikritsis, D.; Koutsos, V.; McCarthy, E. D.; Ó Brádaigh, C. M. Novel Carbon-Fibre Powder-Epoxy Composites: Interface Phenomena and Interlaminar Fracture Behaviour. *Compos. Part B Eng.* **2019**, *174* (January), 107012. https://doi.org/10.1016/j.compositesb.2019.107012.

(3) Bhattacharya, M. Polymer Nanocomposites-A Comparison between Carbon Nanotubes, Graphene, and Clay as Nanofillers. *Materials (Basel).* **2016**, *9*, 1–35. https://doi.org/10.3390/ma9040262.

(4) Li, Q.; Zaiser, M.; Blackford, J. R.; Jeffree, C.; He, Y.; Koutsos, V. Mechanical Properties and Microstructure of Single-Wall Carbon Nanotube/Elastomeric Epoxy Composites with Block Copolymers. *Mater. Lett.* **2014**, *125*, 116–119. https://doi.org/10.1016/j.matlet.2014.03.096.

(5) Brzozowska, A. M.; Parra-Velandia, F. J.; Quintana, R.; Xiaoying, Z.; Lee, S. S. C.; Chin-Sing, L.; Jańczewski, D.; Teo, S. L. M.; Vancso, J. G. Biomimicking Micropatterned Surfaces and Their Effect on Marine Biofouling. *Langmuir* **2014**, *30*, 9165–9175. https://doi.org/10.1021/la502006s.

(6) Balzer, B. N.; Micciulla, S.; Dodoo, S.; Zerball, M.; Gallei, M.; Rehahn, M.; Klitzing, R. V; Hugel, T. Adhesion Property Profiles of Supported Thin Polymer Films. *ACS Appl. Mater. Interfaces* **2013**, *5*, 6300–6306. https://doi.org/10.1021/am4013424.

(7) Duarte, A. P.; Coelho, J. F.; Bordado, J. C.; Cidade, M. T.; Gil, M. H. Surgical Adhesives: Systematic Review of the Main Types and Development Forecast. *Prog. Polym. Sci.* **2012**, *37*, 1031–1050. https://doi.org/10.1016/j.progpolymsci.2011.12.003.

(8) Giannotti, M. I.; Vancso, G. J. Interrogation of Single Synthetic Polymer Chains and Polysaccharides by AFM-Based Force Spectroscopy. *ChemPhysChem* **2007**, *8*, 2290–2307. https://doi.org/10.1002/cphc.200700175.

(9) Neuman, K. C.; Nagy, A. Single-Molecule Force Spectroscopy: Optical Tweezers, Magnetic Tweezers and Atomic Force Microscopy. *Nat. Methods* **2008**, *5*, 491–505. https://doi.org/10.1038/nmeth.1218.

(10) Radiom, M.; Maroni, P.; Borkovec, M. Influence of Solvent Quality on the Force Response of Individual Poly(Styrene) Polymer Chains. *ACS Macro Lett.* **2017**, *6*, 1052–1055. https://doi.org/10.1021/acsmacrolett.7b00652.

(11) Kienle, S.; Gallei, M.; Yu, H.; Zhang, B.; Krysiak, S.; Balzer, B. N.; Rehahn, M.; Schlüter, A. D.; Hugel, T. Effect of Molecular Architecture on Single Polymer Adhesion. *Langmuir* **2014**, *30*, 4351–4357. https://doi.org/10.1021/la500783n.

(12) Zhang, B.; Shi, R.; Duan, W.; Luo, Z.; Lu, Z.-Y.; Cui, S. Direct Comparison between Chemisorption and Physisorption: A Study of Poly(Ethylene Glycol) by Means of Single-Molecule Force Spectroscopy. *RSC Adv.* **2017**, *7*, 33883–1. https://doi.org/10.1039/c7ra05779b.

(13) Xia, W.; Hsu, D. D.; Keten, S. Dependence of Polymer Thin Film Adhesion Energy on Cohesive Interactions between Chains. *Macromolecules* **2014**, *47*, 5286–5294. https://doi.org/10.1021/ma5006974.

(14) Pukánszky, B. Interfaces and Interphases in Multicomponent Materials: Past, Present, Future. *Eur. Polym. J.* **2005**, *41*, 645–662. https://doi.org/10.1016/j.eurpolymj.2004.10.035.

(15) Vázquez-Moreno, J.; Sánchez-Hidalgo, R.; Sanz-Horcajo, E.; Viña, J.; Verdejo, R.; López-Manchado, M. Preparation and Mechanical Properties of Graphene/Carbon Fiber-Reinforced Hierarchical Polymer Composites. *J. Compos. Sci.* **2019**, *3*, 30. https://doi.org/10.3390/jcs3010030.

(16) Ou, Y.; González, C.; Vilatela, J. J. Interlaminar Toughening in Structural Carbon Fiber/Epoxy Composites Interleaved with Carbon Nanotube Veils. *Compos. Part A Appl. Sci. Manuf.* **2019**, *124*, 105477. https://doi.org/10.1016/j.compositesa.2019.105477.

(17) Lattime, R. R. Styrene-Butadiene Rubber. In *Van Nostrand's Encyclopedia of Chemistry*; Considine, G. D., Ed.; Wiley: Hoboken, 2005.

(18) McClements, J.; Buffone, C.; Shaver, M. P.; Sefiane, K.; Koutsos, V. Poly(Styrene-Co-Butadiene) Random Copolymer Thin Films and Nanostructures on a Mica Surface: Morphology and Contact Angles of Nanodroplets. *Soft Matter* **2017**, *13* (36), 6152–6166. https://doi.org/10.1039/c7sm00994a.

(19) McClements, J.; Shaver, M. P.; Sefiane, K.; Koutsos, V. Morphology of Poly(Styrene-Co-Butadiene) Random Copolymer Thin Films and Nanostructures on a Graphite Surface. *Langmuir* **2018**, *34*, 7784–7796. https://doi.org/10.1021/acs.langmuir.8b01020.

(20) Lasseuguette, E.; McClements, J.; Koutsos, V.; Schäfer, T.; Ferrari, M.-C. Ionic Liquid Mediated Surface Micropatterning of Polymer Blends. *J. Appl. Polym. Sci.* **2018**, *135*, 46109. https://doi.org/10.1002/app.46109.

(21) Shafi, A. S.; McClements, J.; Al-Baijan, I.; Abou-Saleh, R. H.; Moran, C.; Koutsos, V. Probing Phospholipid-Microbubbles by Atomic Force Microscopy to Quantify Bubble Mechanics and Nanostructural Shell Properties. *Colloids Surfaces B Biointerfaces* **2019**, *181*, 506–515. https://doi.org/10.1016/j.colsurfb.2019.04.062.

(22) Halperin, A.; Zhulina, E. B. On the Deformation Behavior of Collapsed Polymers. *Europhys. Lett.* **1991**, *15*, 417–421.

(23) Haupt, B. J.; Senden, T. J.; Sevick, E. M. AFM Evidence of Rayleigh Instability in Single Polymer Chains. *Langmuir* **2002**, *18*, 2174–2182. https://doi.org/10.1021/la0112514.

(24) Brochard-Wyart, F.; De Gennes, P. G.; Léger, L.; Marciano, Y.; Raphael, E. Adhesion Promoters. *J. Phys. Chem.* **1994**, *98*, 9405–9410. https://doi.org/10.1021/j100089a009.

(25) Jones, R. A. L.; Richards, R. W. *Polymers at Surfaces and Interfaces*; Cambridge University Press: Cambridge, 1999. https://doi.org/10.1016/B978-0-08-026305-2.50007-3 U6 - http://www.sciencedirect.com/science/article/pii/B9780080263052500073 M4 - Citavi.

(26) Misra, S.; Fleming, P. D.; Mattice, W. L. Structure and Energy of Thin Films of Poly-(1,4-Cis-Butadiene): A New Atomistic Approach. *J. Comput. Mater. Des.* **1995**, *2*, 101–112. https://doi.org/10.1007/BF00701616.

(27) Koutsos, V.; Haschke, H.; Miles, M. J.; Madani, F. Pulling Single Chains out of a Collapsed Polymer Monolayer in Bad-Solvent Conditions. *MRS Proc.* **2002**, *734*, B1.6. https://doi.org/10.1557/PROC-734-B1.6.

(28) Cui, S.; Liu, C.; Zhang, W.; Zhang, X.; Wu, C. Desorption Force per Polystyrene Segment in Water. *Macromolecules* **2003**, *36*, 3779–3782. https://doi.org/10.1021/ma034090e.

(29) Williams, R.; Goodman, A. M. Wetting of Thin Layers of SiO2 by Water. *Appl. Phys. Lett.* **1974**, *25*, 531–532. https://doi.org/10.1063/1.1655297.

(30) Harrison, A. J.; Corti, D. S.; Beaudoin, S. P. Capillary Forces in Nanoparticle Adhesion: A Review of AFM Methods. *Part. Sci. Technol.* **2015**, *33*, 526–538. https://doi.org/10.1080/02726351.2015.1045641.

(31) Welch, D.; Lettinga, M. P.; Ripoll, M.; Dogic, Z.; Vliegenthart, G. A. Trains, Tails and Loops of Partially Adsorbed Semi-Flexible Filaments. *Soft Matter* **2015**, *11*, 7507–7514. https://doi.org/10.1039/c5sm01457c.

(32) Grebíková, L.; Whittington, S. G.; Vancso, J. G. Angle-Dependent Atomic Force Microscopy Single-Chain Pulling of Adsorbed Macromolecules from Planar Surfaces Unveils the Signature of an Adsorption-Desorption Transition. *J. Am. Chem. Soc.* **2018**, *140*, 6408–6415. https://doi.org/10.1021/jacs.8b02851.

(33) Shojaei, A.; Faghihi, M. Physico-Mechanical Properties and Thermal Stability of Thermoset Nanocomposites Based on Styrene-Butadiene Rubber / Phenolic Resin Blend. *Mater. Sci. Eng. A* **2010**, *527* (4–5), 917–926. https://doi.org/10.1016/j.msea.2009.10.022.

(34)   Owens, D. K.; Wendt, R. C. Estimation of the Surface Energy of Polymers. *J. Appl. Polym. Sci.* **1969**, *13*, 1741–1747.

(35)   Schultz, J.; Tsutsumi, K.; Donnet, J.-B. Surface Properties of High-Energy Solids. II Determination of the Nondispersive Component of the Surface Free Energy of Mica and Its Energy of Adhesion to Polar Liquids. *J. Colloid Interface Sci.* **1977**, *59*, 277–282.

(36)   Kozbial, A.; Trouba, C.; Liu, H.; Li, L. Characterization of the Intrinsic Water Wettability of Graphite Using Contact Angle Measurements: Effect of Defects on Static and Dynamic Contact Angles. *Langmuir* **2017**, *33*, 959–967. https://doi.org/10.1021/acs.langmuir.6b04193.

(37)   Narayan, S.; Day, J.; Thinakaran, H.; Herbots, N.; Bertram, M. E.; Cornejo, C. E.; Diaz, T. C.; Kavanagh, K. L.; Culbertson, R. J.; Franscesca, J. A.; Ram, S.; Mangus, M. W.; Islam, R. Comparative Study of Surface Energies of Native Oxides of Si (100) and Si (111) via Three Liquid Contact Angle Analysis Comparative Study of Surface Energies of Native Oxides of Si (100) and Si (111) via Three Liquid Contact Angle Analysis. *MRS Adv.* **2018**, *3*, 3379–3390. https://doi.org/10.1557/adv.2018.473.

(38)   Dupre, A. *Theorie Mechanique de La Chaleur*; Gauthier-Villars: Paris, 1869.

(39)   Falini, G.; Fermani, S.; Conforti, G.; Ripamonti, A. Protein Crystallisation on Chemically Modified Mica Surfaces. *Acta Crystallogr. Sect. D Biol. Crystallogr.* **2002**, *D58*, 1649–1652. https://doi.org/10.1107/S0907444902012763.
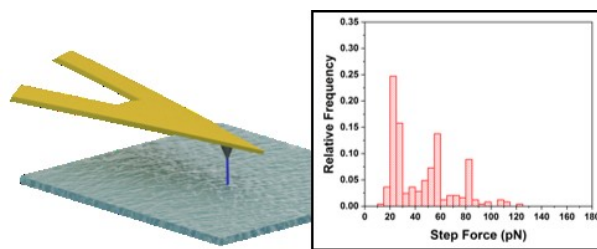
(40)   Li, Z.; Wang, Y.; Kozbial, A.; Shenoy, G.; Zhou, F.; McGinley, R.; Ireland, P.; Morganstein, B.; Kunkel, A.; Surwade, S. P.; Li, L.; Liu, H. Effect of Airborne Contaminants on the Wettability of Supported Graphene and Graphite. *Nat. Mater.* **2013**, *12*, 925–931. https://doi.org/10.1038/nmat3709.

(41)   Keddie, J. L.; Jones, R. A. L. Glass Transition Behavior in Ultra-Thin Polystyrene Films. *Isr. J. Chem.* **1995**, *35*, 21–26. https://doi.org/10.1002/ijch.199500005.

(42)   Miyake, K.; Satomi, N.; Sasaki, S. Elastic Modulus of Polystyrene Film from near Surface to Bulk Measured by Nanoindentation Using Atomic Force Microscopy. *Appl. Phys. Lett.* **2006**, *89*, 031925. https://doi.org/10.1063/1.2234648.

(43)   Ediger, M. D.; Forrest, J. A. Dynamics near Free Surfaces and the Glass Transition in Thin Polymer Films: A View to the Future. *Macromolecules* **2014**, *47*, 471–478. https://doi.org/10.1021/ma4017696.

For table of contents use only